CHARACTERIZING ARC MOTION AND DISTRIBUTION DURING VACUUM ARC REMELTING

C. Rigel Woodside[1] and Paul E. King[1]

[1]National Energy Technology Laboratory;
1450 Queen Avenue SW; Albany, OR 97321-2152, USA

Keywords: VAR; Titanium; Arc; Cathode spots; Distribution; Biot-Savart; Magnetic

Abstract

Previous studies have successfully correlated arc distributions in a vacuum arc remelting (VAR) furnace with the formation of defects during melting, with diffuse arc conditions being the benchmark for high quality ingots. This paper reports on work performed by the National Energy Technology Laboratory directed at determining real time arc distributions. The utilized methodology is based on furnace geometry specific forms of the Biot-Savart Law, which relates internal electric currents to externally measured magnetic fields. The developed measurement system is used to investigate arc behavior during titanium alloy VAR operation. Results are compared to previous experiments investigating arc behavior, as well as theoretical metal vapor arc behavior. It is shown that a magnetostatic single arc model is not sufficient to determine the current distribution inside a VAR furnace at an instant, but it could be used as a tool to detect non-axisymmetric arc distributions during VAR operation.

Introduction

The distribution of arcs versus time is becoming increasingly relevant to the production of high quality large diameter ingots. Arc distribution shifts have previously been correlated to conditions favoring defect formation, with ideal conditions being that of a diffuse arc [1]. This means that arcs distribute evenly across the ingot surface at a time averaged level, leading to a quasi steady and uniform heat input to the melt pool surface. As an indicator that current furnace instrumentation falls short in identifying this condition, it has been shown with high speed cinematography of the arc region that constricted arcs can exist without leaving any evidence of its presence on current and voltage signatures [2].

Defects in ingots can generally said to be solidification related or inclusion related. Maintaining a diffuse arc distribution could be important in preventing solidification defects because distribution shifts could lead to molten pool shape excursions. Inclusion defects are caused by unwanted tramp materials or alloy agent segregation remaining intact during the solidification process, and can come from many sources. One example for this is selective melting away of the shelf resulting in "fall-in" material that later becomes a defect site. The arc has a large thermal effect on the ingot shelf because of its proximity, so arc distribution shifts can again be implicated.

The primary motivation for characterizing arc motion and distribution inside a VAR furnace is to identify and then eventually maintain a desired spatial energy profile so as to ensure a high quality ingot. Currently, there is not a commercially available measurement system capable of detecting the spatial and temporal distribution of arcs during operation. Although optically limited, "seeing" the arc region is possible by measuring the external magnetic fields. An electric

arc produces a magnetic field as described by Maxwell's equations which relate an electric current density to a diverging magnetic flux density. Thus, an arc creates a magnetic flux at a distance which changes dependent on how far away that arc is.

Vacuum Arc Behavior

A vacuum arc refers to an electrical discharge between a cathode and an anode at pressures low enough that the conduction path is sustained by vaporization and ionization of the electrode rather than the ambient gas. The ionized particles constitute the metal vapor plasma which exists between the cathode and anode. In VAR the electrode is the cathode (V-) and the ingot pool is the anode (V+), so electrons flow from the electrode to the melt pool. Generally, the electrical discharge emanates from cathode spots which are small and mobile zones which eject ions and material from the electrode. For titanium, it is reported that a given cathode spot will split into multiple spots once the current exceeds about 70 Amps [3].

The typical VAR electrode, which conducts thousands of Amps, will therefore be expected to have numerous cathode spots. From a measurement stand point it is important to know whether these individual spots cluster and remain collinear which, from a distance, would look like a single arc. Or the individual spots might behave individually, creating the impression at a distance of multiple arcs. Specific to VAR arcs, high speed cinematography has been used to study the electrode gap region. In a VAR furnace it has been observed that cathode spots tend to move around in ill-defined clusters, separating and coalescing with retrograde motion. Although the position of an individual cathode spot was largely random, it was reported that there was a general trend for the spots to form near the center of the electrode and then move in the radial direction, before extinguishing [4].

Methodology

Theory

The basis for determining arc location and in turn distribution is the relationship between a current density and a magnetic flux density. The relationship is shown in equation (1), known as the Maxwell-Ampere equation.

$$\nabla \times \vec{B} = \mu\left[\vec{J} + \frac{\partial \vec{D}}{\partial t}\right] \tag{1}$$

In this equation, B is the magnetic flux density, μ is the magnetic permeability of the medium through which the field is diverging, J is the current density, and $\partial D/\partial$t is the rate of change of the electric field which is sometimes referred to as the displacement current. The terms are vectors. Magnetic permeability is a material property and the materials of construction in the typical VAR furnace have the same permeability. Also, most VAR furnaces operate using direct current, which simplifies the equation by eliminating the displacement current term. The complexity in using this equation to find an arc, though, arises because the movement of the arc also causes the current paths in the rest of the furnace to change. Thus, the magnetic flux density external to a furnace is a function of these sources in addition to the flux generated by an arc.

Finite Element Modeling

To describe the complex relationship of the current paths, COMSOL Multiphysics, a general finite element analysis (FEA) software package, was utilized. COMSOL solves problems using the finite element method with partial differential equations.

First, a 3-D CAD model of the furnace and the experimental set-up, including sensor location, is created. Multiple models are needed to account for varying ingot heights during a melt. At a given instant, it was assumed that only a single arc (cluster of cathode spots) exist; although this assumption is questionable, this formulation allows for a unique determination of arc location from a single sensor as detailed below. Both the arc diameter and electrode gap length were set to 25 mm. Given typical cathode spot densities, it could be possible to fit all the expected spots in a diameter less than 25mm. A larger cluster size was also considered, but this was avoided because the FEA as utilized would determine a non-uniform current profile within the cluster that is biased toward the center of the furnace, which complicates the prediction and has no known theoretical basis. The electrical conductivity in the electrode gap outside of the arc was set to a value near zero, which essentially forces all of the current through the arc in the model. This also is a questionable assumption as there likely is a more diffuse yet non-trivial ion current through the plasma region. Without quantitative knowledge of this current, it was decided to neglect this effect for the sake of simplicity. In reality, previous studies indicate that there is diffuse conduction of some of the current through this space by means of the plasma. For one, it is well known that the total power applied to a VAR furnace does not explain the melting rates observed. In addition, attempts have been made to track the current movement from the electrode to the crucible by measuring the surface voltage profile on the crucible. It was found that only 63% of the total current appeared to travel through the ingot pool, with the remaining balance traveling directly from the electrode to the crucible [5].

Next, the entire model geometry is meshed to create the discrete finite elements. In solving the problem, a finite element electrostatic equation is first utilized in order to determine the current density throughout the geometry. The electrostatic solution is then input into the magnetostatic finite element version of equation (1) which solves for the magnetic flux density. The output of each model is the magnetic flux density at each sensor location for various arc location scenarios. Thermal or magneto-hydro-dynamic processes are not modeled in the FEA. These processes are important to VAR operation, but can be neglected in the model because the processes will not have an arc location independent effect on the external magnetic flux density.

There have been previously published studies using magnetic flux density measurements to characterize VAR arc conditions by R.M. Ward [6]. Ward's technique also involved using magnetostatic finite element modeling to solve for the magnetic flux density vector at a sensor’s location for various single arc location simulations. The magnetic flux density simulation results were then compared to the measurements and a most likely arc position was determined via regression.

In this paper, we take a modified approach and show there is a deterministic solution for a single arc's location using a single magnetic flux density vector measurement. A continuous solution was desired so that the predicted arc positions would not be mathematically limited to the arc locations that were simulated. The realization of such a solution makes excessive finite element simulations unnecessary.

Deterministic Equations

For the magnetostatic formulation of equation (1), magnetic flux density at a point can be analytically solved for using what is known as the Biot-Savart Law as stated in equation (2).

$$B(P) = \frac{\mu_o}{4\pi} \int \frac{Ix\hat{\eta}}{\eta^2} dI \tag{2}$$

where *B(P)* is the magnetic flux density at a point in space (Teslas). The integration is along the current path in the direction of flow, *dI* is an element of length (m) along the current *I* (Amps), and η is the vector from the source to the point. μ_0 is the permeability of vacuum. This equation is also applicable when dealing with slow varying currents. Indeed, electrical processes changing in the 60Hz range can be solved for using the Biot-Savart Law without introducing much error [7].

Further simplification can be performed in the case that the electric current has known boundaries. The magnetic field emanating from an arc pointed in the axial direction will only have a radial and azimuthal component in a plane normal to and intersecting the center of that arc. Using vector superposition of the arc's vector and a vector in the same direction which is unaffected by movement of the arc, we can approximate the relation of the magnetic flux measurement to a single arc position in a VAR furnace with equations (3) and (4).

$$B_x = m_x I\left(\frac{\sin(\Theta_a)}{d_a} - a\right) \tag{3}$$

$$B_y = m_y I\left(\frac{\cos(\Theta_a)}{d_a} - b\right) \tag{4}$$

where B_x and B_y are components of the magnetic flux density at a sensor's location using a Cartesian coordinate system, θ_a is the angle from the sensor to the arc, d_a is the distance from the sensor to the arc, and *I* is the total circuit current in Amps. The constants *a, b,* m_x, and m_y are needed to compensate for the finite arc length, and furnace geometry. If the constants are known then there are two equations and two unknowns, θ_a and d_a. After inverting equations (3) and (4) to solve for these, two solutions for the location of a current are found for a given magnetic flux density vector. However, one can be eliminated because it is on the opposite side of the sensor than the furnace.

In the case of an ideal coaxial furnace, the constants *a* and *b* can be readily solved for by considering that both components of the external magnetic flux are zero in the case of a centered arc. Thus, with a coaxial furnace, one of these terms is 0 and the other is $1/d_a$, depending on the sensor orientation. One way to find the constants m_x, and m_y is to use the FEA. The FEA, as discussed above, is used to create a data set of *B* versus *I,* θ_a, and d_a. A least squares regression is performed to fit this data set to equations (3) and (4) in order to find the parameters, m_x and m_y.

It was found the predictions of arc locations using the deterministic equations were within about 30mm of simulated arc positions using the FEA, with exception to when the arc was on the opposite side of the furnace and furthest from the sensor. At this location the error of the linearization was closer to 80mm. Averaging 4 sensor predictions from sensors on opposite sides of the furnace improved the prediction by suppressing the errors from an individual sensor, so that all the predictions were within about 30mm of the simulated arc position. As the ingot forms

and the electrode gap moves away from the sensor plane, there is an increasing error in using the same equations. Still, averaging 4 individual sensor predictions using the deterministic equations gives an arc position determination with agreement to FEA simulations to within about +/- 30mm for about 150mm of distance along the furnace axis.

Experimental Set-up

Commercially available multi-axis Hall Effect sensors were chosen to measure the external magnetic fields. These multi-axis sensors have three closely spaced, orthogonally oriented sensor elements that can be used to determine the direction of the magnetic flux in addition to sensing the intensity of the magnetic flux. Eight multi-axis Hall effect sensors were externally attached to a commercial coaxial VAR at ATI-Allvac's Albany, Oregon facility in two arrays of four sensors each. Magnetic Flux density data was recorded from these sensors during several Titanium alloy heats. In addition to the magnetic flux density data, furnace current, voltage, and stirring coil current were acquired. For the results reported in this paper, data were recorded at a sampling rate of 3.7kHz

To account for the magnetic field created by the stirring coils, data were collected prior to striking an arc but with the coils on. The magnetic data were then fit to the measured stirring coil current so that an offset as a function of stirring coil current could be determined. This offset function was then subtracted from the magnetic flux density measurements in the post processing. To estimate the electrode gap position along the axis during the run, an electrode based approach was utilized. This took into account the dimensions and density of the electrode, as well as ram position and electrode load cell data.

Results and Discussion

A single final Ti alloy melt is presented. These results are for an arbitrary amount of data acquired when the electrode gap plane was determined to be near a plane containing 4 of the sensors. The exact operation parameters such as melt rate for this run are proprietary to ATI-Allvac, but some generalities can be said. The data presented is for a 91.44 cm diameter final titanium alloy melt having amperage greater than 30kA, voltage 30 to 50 volts, and low stirring with moderate reversal times. The electrode was 76.2 cm in diameter. Analyzing a single cross section gives a snapshot, but for a given operation condition, arc behavior has previously found to be fairly consistent from run to run [8].

Utilizing the arc location equations, the x-y arc position can be calculated for each sensor, as well as the average of these locations. The average is the average of the predictions, as opposed to an averaging of the measured signals. Arc location data was investigated at the full time scale acquired, and it was found that the significant activity appeared to be occurring at the lower frequencies. So for noise reduction purposes, the test data was processed through a low pass filter having a cut-off frequency at 25Hz. The data was then reduced to 50Hz.

Arc Location

If the utilized assumptions are correct, we would expect all of the sensor's predictions to be in agreement in their arc location predictions at an instant and it would be expected that the predicted arc locations would cover the entire surface of the electrode if one looked at long enough of a duration. Figure 1 shows the average arc location predictions over 720 seconds of

melt time as well as predictions from each sensor for 3 instances chosen to demonstrate different arrangements of predictions seen in the data.

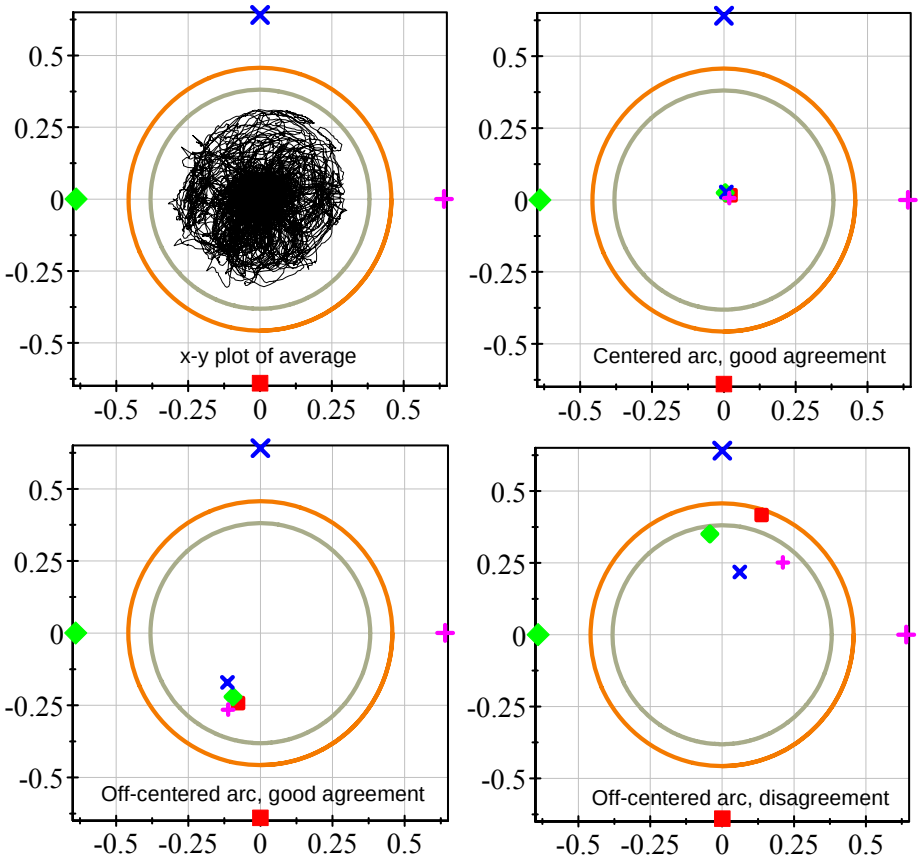

Figure 1 : The average of the predicted arc locations over 720 seconds of melt time (top-left) and a comparison of arc location predictions from the individual sensors at 3 instances; The dimensions are in meters, and the markers represent actual sensor location in addition to the location prediction. The outer circle is the crucible, and the inner circle is the electrode.

In the top-left of figure 1, it can be seen that the average prediction coverage area is close to the electrode size, with the prediction's coverage area being smaller in radius by about 75mm. It should be noted that the plot shows the center of the predicted arc's location. Therefore, if the arc has a radius of about 75mm, then the predicted arc locations would cover the entire surface. Not shown in the figure is x-y plots from the individual sensors. These were found to have a slightly larger total coverage area compared to the average, but still smaller than the electrode's surface.

As can be seen in figure 1, the agreement between predictions varies. Yet overall the predictions amongst sensors showed fairly good agreement with the average distance from a single sensor's prediction to the average prediction being about 30 mm over the course of the data presented. Finding general agreement between predictions is in contrast to earlier work, in which the sensors disagreed and appeared to predict radial oscillations at 360 Hz [8]. Examining further, the disagreement was not consistent at a given position, as might be expected if disagreement were due to a systematic measurement error or a systematic error associated with neglecting the diffuse plasma current. The disagreement can, though, be explained by multiple arcs.

Additionally, agreement between sensors does not mean there is a single arc at that instant. For example, multiple arcs that are symmetric about the center of the furnace will have nearly the same magnetic signature at a distance on all sides of the furnace as that of a single centered arc and thus the predicted arc locations with the single arc approach will be identical for both cases and for all sensors. On the other hand, non-centered multiple arcs will leave a different signature on different sides of the furnace. So a furnace with multiple arcs should generally yield better agreement between sensor predictions for centered multiple arc scenarios versus non-centered multiple arc scenarios utilizing this methodology. For this data, agreement was better for the centered arc predictions, compared to the non centered predictions. This supports the case for multiple arc phenomena.

It is believed that the agreement pattern observed indicates multiple arcs (cathode spot clusters) at any given instant and even possibly at most instances. This means determination of motion and distribution with the single arc model will be inaccurate. Still, in terms of generally characterizing arc motion and distribution the single arc model may be an effective means to identify diffuse, constricted, and other arc behavior.

Arc Position and Motion

The motion of the arcs appear to have significant radial as well as azimuthal components. Figure 2 shows the calculated radial position versus time, as well as a cumulative angle for the arc's position versus time. This term, denoted arc rotations, was found by assigning a rotation value of 0 to the initial data point and then accumulating the changes in the determined polar angles for the remaining data points.

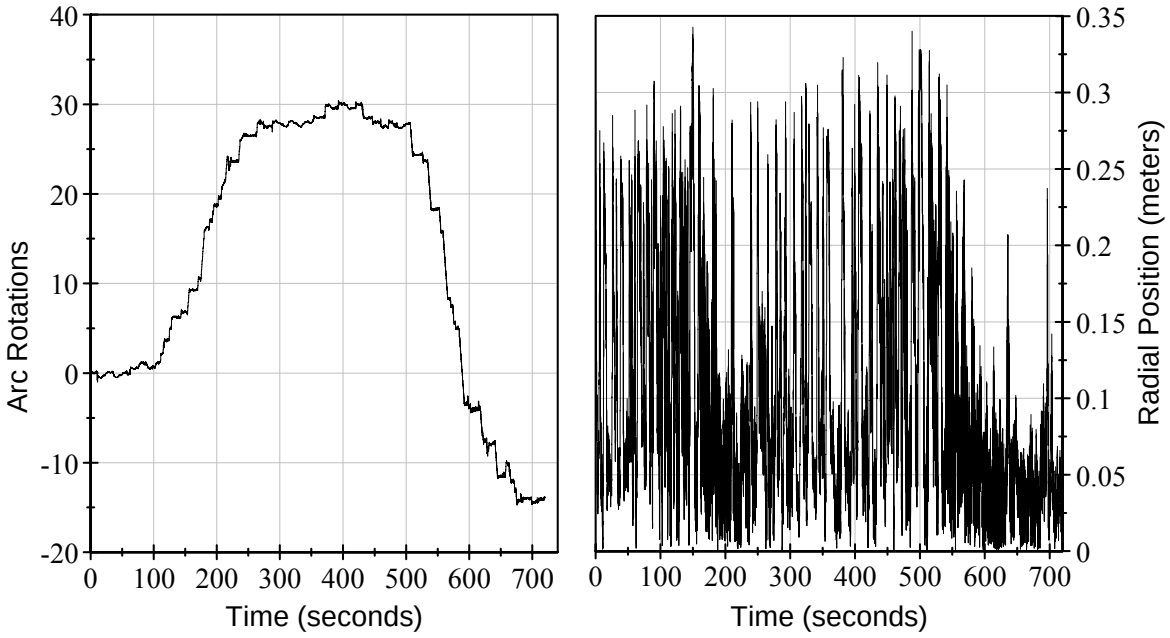

Figure 2: Arc rotations about the center of the furnace axis when viewed from above (left) and radial position (right) of the average predicted arc location. One arc rotation is 2π radians, and the positive direction is clockwise.

The radial motion appears to vary from periods of significant motion, to periods of less radial motion. Performing a Fast Fourier Transform (FFT) of this data, three frequencies appear to play the largest role, one corresponding to a time period of about 1 second, and two lower frequencies

at intermediate time scales between 5 and 20 seconds. All these frequencies also appear in the furnace's current and voltage data, though it is unknown at this time whether these frequencies arise from the furnace's power supply, or whether arc dynamics are causing these frequencies to appear in those signals. The low radial motion at the end of the data shown in Figure 2 also appears to be accompanied by slightly lower noise in the current signal.

It was expected that reversal of the stirring coil might cause arc rotation reversal, but this does not seem to be the case. Instead, the arc rotates about the center of the furnace in a clockwise direction for the first half of the data presented, followed by an overall counter clockwise rotation for the remainder of the data. When the predicted arc position is rotating about the center, it does so at time scales between 1 to 20 seconds per rotation. Ward also found that there may be an ensemble azimuthal arc rotation, but at a longer time scale in the range of 20 to 40 seconds per rotation [6]. Additionally, he also observed the switching from clockwise to counter clockwise rotation at even longer time scales. The shorter time scales observed here for rotation may be due to the higher melting rate utilized when melting Ti, characteristics of the materials melted, characteristics of the power supplies, or it may be related to the stirring coil. However, it does not appear that the stirring coil has a large impact on the arc dynamics for these experiments at least in terms of its polarity reversal.

The average determined velocity varies but does not show any significant time varying pattern. The average velocity for the data presented is generally between 0 and 0.5 m/s, with an average of about 0.25 m/s. There are also outliers, with a maximum velocity of 2.4 m/s calculated for the data evaluated.

Arc Distribution

To visualize a time averaged distribution, a 2-D histogram of the x-y position data was performed. The x-y square bin size was selected to be 12.7mm. Figure 3 shows an overhead view of the furnace, with the color intensity corresponding to the number of arc predictions found in each bin.

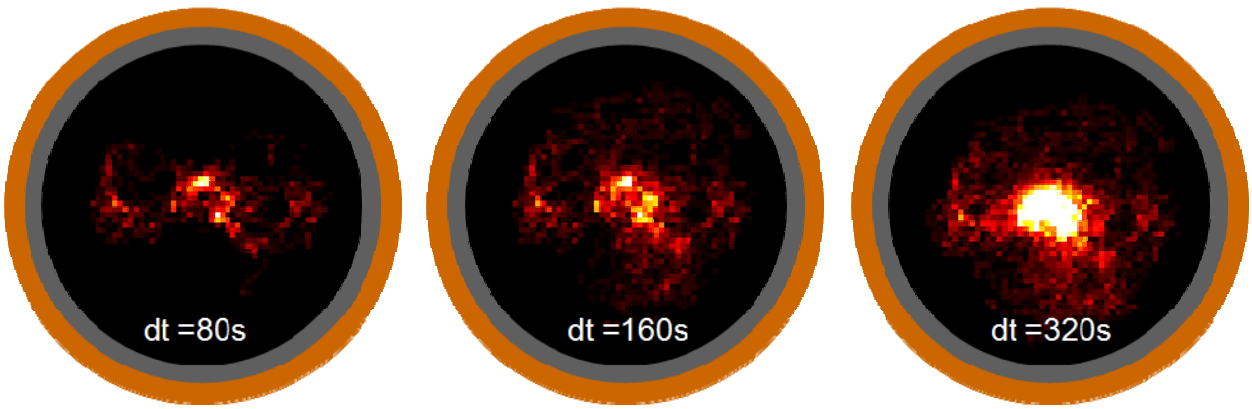

Figure 3 : Overhead view of the predicted arc distribution in the VAR furnace over increasingly long time scales. Color intensity corresponds to the number of arc location predictions in each location bin. The dark circle is the electrode.

It can be seen that the arc predictions are concentrated in the center of the furnace. However, this does not necessarily mean arcs were mostly located there. For example, if the prevailing

condition consisted of multiple arcs near the edges that were symmetric about the center of the furnace, then the utilized single arc method would also yield a distribution plot that looks like figure 3. Therefore, this method is of limited use in determining an accurate arc distribution versus radial position. Still, the method may be useful as a diagnostic in order to avoid non-axisymmetric behavior during operation. Such behavior would result in the distribution shifting away from the center, or would show up in the visualization as "hot spots" in certain locations. If such states were observed, corrective control action might then be able to return the furnace to the desired arc condition.

Conclusions

This paper describes the instrumentation and analysis techniques for characterizing arc behavior using externally mounted magnetic flux density sensors. The following conclusions can be made as a result of this work.

1. The disagreement of arc location predictions at an instant from independently calculated sensors is consistent with the presence of multiple arcs (multiple cathode spot clusters) acting somewhat independent of one another. Therefore, the single arc model presented is not sufficient to determine the current density within the furnace at an instant.

2. Arc motion results show a radial component operating at several characteristic time scales in the 1 to 20 seconds per cycle range. The frequencies appear to be equivalent to frequencies observed in the current and voltage waveforms. The radial motion also appears to occur less frequently for certain sections of the data analyzed.

3. Arc motion results show an azimuthal component with a long period of clockwise rotation about the center of the furnace, followed by a period of no net rotation, followed by a long period of counter clockwise rotation. When rotating, the time scale for a single rotation about the axis is typically in the 1 to 20 second range.

4. The single arc method may be sufficient to use a diagnostic tool to ensure axisymmetric behavior during melting. The methodology described in this paper is simple enough that real time monitoring is currently possible.

This research may also provide insight into the role of stirring coils in arc motion and distribution. For example, the reversal of the current in the coil did not seem to effect arc behavior for the data examined, though the level of stirring for these tests is considered to be low by industry standards.

Ultimately, as the technique becomes more sophisticated to allow for multiple arcs, magnetic field measurements could lead to maps of the distribution of energy into the surface of the melt pool. This information could be used to improve VAR solidification models. Currently, these models assume a certain distribution of current density into the melt pool. The knowledge of arc distribution during VAR operations, and thus current density distribution, is information needed to make more realistic solidification models of an actual melt possible.

Acknowledgements

A portion of this work was supported though a cooperative research and development agreement between the United States Department of Energy's National Energy Technology Laboratory and the Specialty Metals Processing Consortium. The authors would also like to thank and acknowledge the help from the personnel at ATI-Allvac's Albany facility. Thanks to Chris Nordlund for facilitating the experiments, as well as helpful discussions about VAR operation. Thanks to Steve Henrickson for his help in interfacing the measurement system to the existing furnace instrumentation. Thanks to Mike Whaley for compiling internally acquired data so that the ingot height could be calculated as a function of time for the data examined. Finally, thanks to the rest of the crew for help in scheduling data retrieval, and putting up with a researcher in an industrial setting.

References

[1] Zanner, F., Williamson, R., and Erdmann, R., 2005, "On the Origin of Defects in Var Ingots," Proc. International Symposium on Liquid Metal Processing and Casting, Santa Fe, NM, USA, pp. 13.

[2] Zanner, F. J., Adasczik, C., Obrien, T., and Bertram, L. A., 1984, "Observations of Melt Rate as a Function of Arc Power, Co Pressure, and Electrode-Gap During Vacuum Consumable Arc Remelting of Inconel 718," Metallurgical Transactions B-Process Metallurgy, 15(1), pp. 117-125.

[3] Boxman, R. L., Sanders, D. M., and Martin, P. J., 1995, Handbook of Vacuum Arc Science and Technology : Fundamentals and Applications, Noyes Publications, Park Ridge, N.J., U.S.A.

[4] Zanner, F. J., and Bertram, L. A., 1983, "Behavior of Sustained High-Current Arcs on Molten Alloy Electrodes During Vacuum Consumable Arc Remelting," Ieee Transactions on Plasma Science, 11(3), pp. 223-232.

[5] Williamson, R. L., Shelmidine, G. J., and Maroone, J. P., 2005, "Current Profiles During Var of Ti-6al-4v," Proc. International Symposium on Liquid Metal Processing and Casting, Santa Fe, NM, USA, pp. 29.

[6] Ward, R. M., Daniel, B., and Siddall, R., 2005, "Ensemble Arc Motion and Solidification During the Vacuum Arc Remelting of a Nickel-Based Superalloy," Proc. International Symposium on Liquid Metal Processing and Casting, pp. 49.

[7] Griffiths, D., and College, R., 1999, Introduction to Electrodynamics, Prentice Hall Englewood Cliffs, NJ.

[8] Woodside, R., 2008, "Investigating Arc Behavior in a Dc Vacuum Arc Remelting Furnace Using Magnetic Flux Density Measurements," Master of Science Oregon State University, Corvallis.